# Effect of Emergent Rigid Vegetation on Flow Properties in an Open Channel


**J. R. Khuntia, K. Devi, B. S. Das, K. K. Khatua, and S. Jena**

**Abstract** The flow characteristics in open channels with emerging rigid vegetation are discussed in this paper. By strengthening ecosystem sustainability and restoration, vegetation can be actively exploited as a tool for flood management. Vegetation growing in channels irregularly raises the hydraulic resistance, which can result in energy loss and reduced conveyance capacity. The results of the earlier experiments have been thoroughly investigated regarding the flow resistance produced by uniformly distributed vegetation stems. The vegetation consists of emergent rigid rods replicating stem of a tree. Velocities were measured using 3D acoustic Doppler velocimeters (ADV), with both downward facing and upward facing probes. The magnitude of the longitudinal velocities was found to decrease significantly behind the vegetative stem. Due to the presence of turbulence, the transverse and vertical velocities were high. According to the findings, vegetation density, stem diameter, vegetation length and flow depth all affect flow resistance. Additionally, it has been seen that as vegetation density increased, the flow rate reduced. The relationships between friction factor ($f$) and Manning's coefficient ($n$) with the independent non-dimensional geometric and roughness parameters have been demonstrated. Experimental data sets of NITR and past researchers have been taken for developing a new mathematical relationship for roughness in terms of non-dimensional parameters.

J. R. Khuntia (✉) · K. Devi
Department of Civil Engineering, Chaitanya Bharathi Institute of Technology (A), Hyderabad 500075, India
e-mail: jnanaranjan444@gmail.com; jnanaranjan_civil@cbit.ac.in

K. Devi
e-mail: kamalinidevi1@gmail.com; kamalinidevi_civil@cbit.ac.in

B. S. Das
Department of Civil Engineering, National Institute of Technology Patna, Patna 800005, India
e-mail: bsd.nitrkl@gmail.com; bsd.ce@nitp.ac.in

K. K. Khatua · S. Jena
Department of Civil Engineering, National Institute of Technology Rourkela, Rourkela 769008, India
e-mail: kkkhatua@nitrkl.ac.in

S. Jena
e-mail: sjena@nitrkl.ac.in



P. V. Timbadiya et al. (eds.), *Fluid Mechanics and Hydraulics*, Lecture Notes in Civil Engineering 314, https://doi.org/10.1007/978-981-19-9151-6_1

The mathematical expression has been proved to match well with the experimental data sets and found to be better as compared to that of the conventional equations.

**Keywords** Open channel · Flow resistance · Friction factor · Manning's coefficient · Rigid vegetation

## 1 Introduction

In main channels, floodplains and wetland water areas, vegetation like grasses, bushes and mangroves often grow. They increase the shear stress at the channel bed which further increases the hydraulic resistance. As a result, the carrying capacity of an open channel flow is diminished which causes better sediment deposition and restricts the potential of flow. Vegetation plays a crucial role in the movement of sediments and regulation of ecosystems in coastal and riverine areas. Therefore, the presence of vegetation is essential for the restoration of riverine ecosystems. Ecological, morphological, hydrological, and water quality considerations are just a few of the multifarious factors that contribute to the overall restoration process [1]. Analyzing the hydrodynamics of naturally occurring rivers with vegetation is challenging and difficult. However, vegetation affects flow resistance from a hydraulic perspective and reduces the likelihood of flooding. Depending on the flow depth, vegetation may be emergent or submerged. Emergent vegetation is defined as having the rest of its stems above the water's surface and flowing water up to a certain height of the stem.

The type and density of the vegetation, together with the depth and speed of the flow, all affect how the river behaves when it passes through vegetation. Due to the bending of streamlines driven on by the vegetation, the Manning's n roughness or Darcy–Weisbach friction factor can change with the area of mean channel velocity [2]. Additionally, vegetation prevents erosion by connecting soil with roots, decreasing runoff velocity, reducing flux, absorbing the impact of raindrops (i.e., reducing dislodging) and shielding the soil from the sun's and wind's effects (i.e., preventing drying) [3]. The properties of mean flow and turbulence for both rigid and flexible vegetation were examined by Tsujimoto et al. [4]. Vegetation can create complex two-dimensional currents, eddies, and stagnation zones, which can increase friction and obstruct the flow. This type of vegetation-induced turbulence can make it difficult to analyze and understand the hydrodynamics of rivers [5]. Meijer and Van Velzen [6] used steel rods as well as natural reeds for their experiments. Nepf [7] created and evaluated a physical model that predicts the diffusion, vegetation drags and turbulence intensity within emergent vegetation. Under emergent and submerged scenarios, Stone and Shen [8] studied the hydraulic resistance of flow and simulated with cylindrical stems. Ghisalberti and Nepf [9] employed a typical eelgrass meadow model. They claimed that the various vegetation concentrations had an impact on the hydraulic conditions, such as the turbulence patterns and vertex characteristics. Flow with emergent vegetation, the velocity profile is influenced by changes in the density and the orientation of vegetation [10].

The objective of this present paper is to extend the study of emergent vegetation, i.e., effect of flow resistance and drag coefficient with different flow depth and vegetation density. A mathematical model is developed between drag coefficient ($C_D$) and friction factor ($f$), Manning's coefficient ($n$), Reynolds number (Re) and vegetation density ($\lambda$). The variation of $C_D$ against $D/s$, $Re_d$, $Re_h$, Fr and $\lambda$ has been analyzed for model development.

## 2 Theoretical Analysis

### 2.1 Drag Coefficient

The drag force ($F_D$) per fluid mass due to vegetation can be formulated as (Thom [11])

$$F_D = \frac{1}{2}\rho A C_D U^2 \tag{1}$$

where $\rho$ is the density of water, $U$ is the mean velocity of uniform flow, $A$ projected area to the flow and $C_D$ is drag coefficient.

### 2.2 Vegetation Density

The number and spacing between the rods is based upon the vegetation density ($\lambda$). Non-dimensional vegetation density is the product of number of vegetation and area of each stem/rod.

$$\text{Density}, \quad \lambda(\%) = \frac{N\pi D^2}{4} \tag{2}$$

where $D$ is rod/stem diameter (m), $N$ is total number of vegetation per unit area ($m^{-2}$).

### 2.3 Reynolds Number

Two different Reynolds numbers have been used for this study, i.e., Reynolds number considering the diameter of the stem as characteristic length ($Re_d$) and Reynolds number considering the flow depth as characteristic length ($Re_h$).

$$\text{Mathematically}: \ \mathrm{Re_d} = \frac{\mathrm{UD}}{\nu} \ \text{and} \ \mathrm{Re_h} = \frac{\mathrm{Uh}}{\nu} \tag{3}$$

where $h$ is depth of flow (m), $\nu$ is kinematic viscosity ($m^2/s$).

### 2.4 Froude Number

Froude number for each flow depth is defined as:

$$\mathrm{Fr} = \frac{U}{\sqrt{\mathrm{gh}}} \tag{4}$$

## 3 Experimental Setup and Procedures

Experiments were conducted in a recirculating rectangular tilting flume of length 12 m, 0.6 m width and a maximum depth of 0.6 m with longitudinal slope 0.001 at Hydraulic Engineering laboratory of NIT Rourkela. The tilting flume is made of mild steel frame with glass wall at the test reach section. The details of experimentation are in Khuntia [12]; Khuntia et al. [13–16]. Some experimental data sets are also collected from Panigrahi [17] for flow modeling. The layout of the experimental setup used in the present study is shown in Fig. 1. Table 1 shows the geometrical details of the experimental channel section of NITR.

In the present study, cylindrical iron rods of diameter 6.5 mm are used as replica of vegetation (tree) stems. The rods are drilled into the plywood and filled the holes with adhesives to make it watertight for which water will not seep through the holes. The staggered pattern of rods with spacing in each row and column was 10 cm. The

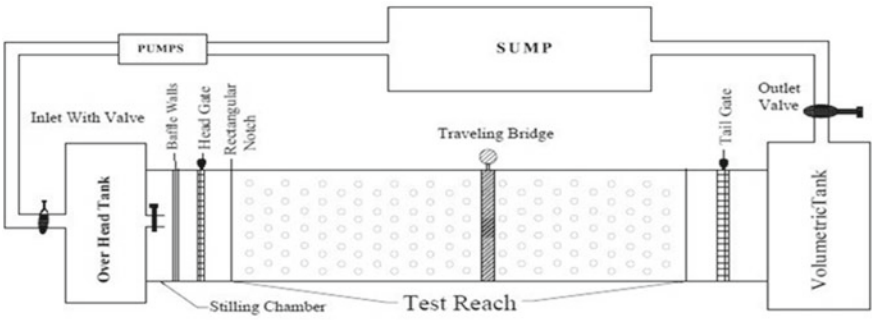


**Fig. 1** Layout of experimental setup, NITR

**Table 1** Geometrical details of the experimental channel section of NITR

| Sl. No. | Particulars | Specifications |
|---|---|---|
| 1 | Channel and geometry type | Straight and rectangular |
| 2 | Channel bottom and top width (B) | 0.6 m |
| 3 | Depth of the flume | 0.75 m |
| 4 | Longitudinal slope (S) | 0.001 |
| 5 | Length of the flume | 12 m |
| 6 | Test reach length | 10 m |
| 7 | Type of bed surface | Rigid cylindrical emergent vegetation |

staggered arrangement of vegetation and arrangement of rigid rods in experimental flume are shown in Fig. 2 and Fig. 3, respectively.

In this study, the important parameters were measured in experimentation, i.e., bed slope, depth of flow, velocity and discharge. To measure the bed slope of the channel, the water is to be ponded by closing the tail gate. Then, the point gauge of least count 0.01 mm was used to measure the depth of water at the two end points along the centre-line of the test reach. The slope of the channel was found by dividing the different in depth of water at two ends to length between two ends. After the measurement, the longitudinal slope or bed slope was found as 0.001. The bed slope was kept constant throughout the experiments. Depth of flow in the channel was measured using a point

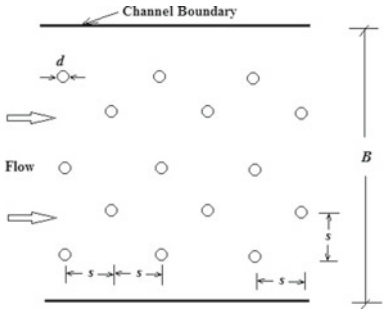


**Fig. 2** Staggered arrangement of vegetation

**Fig. 3** Arrangement of rigid rods as emergent vegetation

**Table 2** Geometric features of vegetation used in NITR channel

| Sl. No. | Particulars | Specifications |
|---|---|---|
| 1 | Type and shape | Emergent rigid and cylindrical |
| 2 | Stem diameter ($d$) | 0.0065 m |
| 3 | Stem length ($l$) | 0.1 m |
| 4 | Spacing each side | 0.1 m |
| 5 | Number of stems | 76/m$^2$ |
| 6 | Test reach length | 10 m × 0.6 m |

gauge fitted with traveling bridge. Local velocities were measured by using three-dimensional 16 MHz micro-ADV (acoustic Doppler velocimeter) at several locations along and across the pre-defined channel sections. The micro-ADV holder was also attached to the traveling bridge on the other side of the point gauge. The discharges were measured using volumetric tank at downstream end of the flume. A vertical piezometer with water table indicator of least count 0.1 cm fitted to the volumetric tank which helps to measure the constant rise of water in it. For this purpose, the passing way of water from volumetric tank to underground sump has been closed by valve. The time of rise in water level in the piezometer is recorded by a stopwatch. The volume of water is the product of volumetric tank area and height of 1 cm water rise in the piezometer. Finally, the discharge is calculated by dividing the volume of water to the time required (in second) for the rise of 1 cm of a particular flow depth. The discharge is thus computed for every experimental run through time rise method. Table 2 shows the geometric features of vegetation used in NITR channel.

## 4 Longitudinal Velocity Profiles

Velocity profiles generally follow the log law profile in case of no vegetation. The effect of bed friction on the shape of the profile is only important near the bed surface where the profile decreases to zero (Stone and Shen [8]).

Velocity at different longitudinal distances along the flow direction was measured by ADV and pitot tube (i.e., where ADV is not accessible) for each experimental run in the rigid vegetated open channel under emergent cases. Velocities were measured at every 0.1 $h$ interval where $h$ is the flow depth. These measured values of velocities were plotted as velocity profiles and is shown in Fig. 4.

From Fig. 4, it is observed that the velocity profiles are mostly uniform over each depth of flow. The magnitude of the velocity is increased with increase in depth of the flow. From experimental data of NITR series, the variations of drag coefficient ($C_D$) with non-dimensional parameters (i.e., $\mathrm{Re_d}$, $\mathrm{Re_h}$, Fr, $f$, $n$) have been plotted in Fig. 5.

From Fig. 5, it has been observed that drag coefficient ($C_\mathrm{D}$) increases with increase in Reynolds number based on stem diameter ($\mathrm{Re_d}$) and Froude number (Fr). But, drag

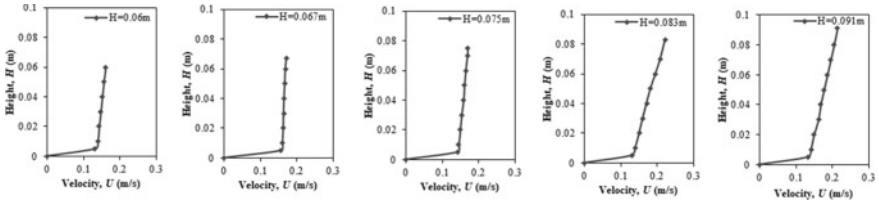


**Fig. 4** Longitudinal velocity profiles of different flow depths (NITR series)

coefficient ($C_D$) decreases with increase in Reynolds number based on flow depth ($Re_h$), friction factor ($f$) and Manning's roughness coefficient ($n$).

## 5 Model Development

Drag coefficient ($C_D$) is an important parameter for every experimental study with vegetation. So, this paper tries to develop a multi-variable regression model by taking some important non-dimensional parameters so that it will help to find out the drag coefficient. For this present model, $C_D$ is taken as dependent parameter and $D/s$, $Re_d$, $Re_h$, Fr and $\lambda$ are taken as independent parameters. The variations of $C_D$ against $D/s$, $Re_d$, $Re_h$, Fr and $\lambda$ have been analyzed for model development.

### *5.1 Multi-variable Regression Analysis*

In this present study, a number of possible single regression models considering different one-to-one relationship (e.g., exponential, power, linear or logarithmic) between dependent parameter and independent parameters were tested. Based on a criterion, the selection of best regression models was achieved with the highest coefficient of determination ($R^2$) values. Five preferred input independent variables have been used for this study since each variable was controlling the drag coefficient. Multi-variable regression analysis compiles these five independent variables to model the dependent variable. Finally, through multi-linear regression analysis, a model has been derived with high coefficient of determination.

The independent variables were determined by using the cross-sectional geometric non-dimensional parameters ($D/s$ and $\lambda$) and hydraulic non-dimensional parameters ($Re_d$, $Re_h$ and Fr). Then, the plot between independent parameters with the dependent parameter has been plotted. From those plots, the relationship of each independent parameter with dependent parameter with high regression coefficient (i.e., $R^2 \approx 0.92$–0.99) has been selected for regression analysis is shown in Fig. 5. Table 3 presents geometric and hydraulic parameters used in this study.

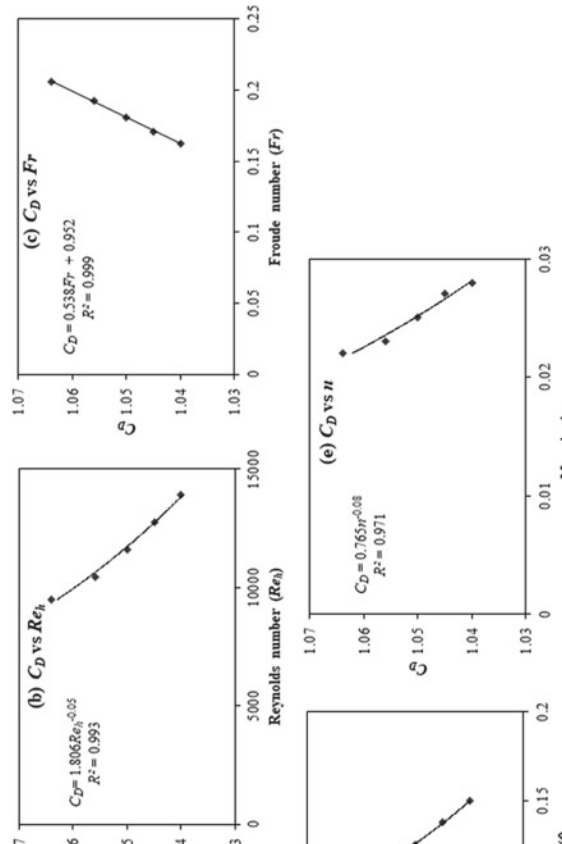


**Fig. 5** Plot between drag coefficient ($C_D$) and influencing parameters of NITR series **a** $C_D$ versus $Re_d$ **b** $C_D$ versus $Re_h$ **c** $C_D$ versus Fr **d** $C_D$ versus $f$ **e** $C_D$ versus $n$

**Table 3** Geometric and hydraulic parameters used in this study

| Series | $D$ (m) | $s$ (−) | $D/s$ (−) | $Re_d$ (−) | $Re_h$ (−) | Fr (−) | λ (%) |
|---|---|---|---|---|---|---|---|
| NITR | 0.0065 | 0.01 | 0.65 | 994–1027 | 9480–13,923 | 0.162−0.206 | 0.25 |
| Kothyari et al. [18] | 0.01 | 0.091 | 0.109 | 4000 | 240,000 | 0.165 | 0.25 |
| Thomson et al. [19] S1 | 0.025 | 0.223 | 0.112 | 14,152 | 183,245 | 1.285 | 0.28 |
| Thomson et al. [14] S2 | 0.025 | 0.135 | 0.185 | 26,054 | 285,547 | 1.45 | 0.3 |
| Stone and Shen [8] S1 | 0.0121 | 0.1446 | 0.0837 | 542–7301 | 5301–71,289 | 0.039−0.522 | 2.2 |
| Stone and Shen [8] S2 | 0.0121 | 0.1448 | 0.0835 | 1338–9762 | 13,067–95,317 | 0.096−0.698 | 6.1 |
| Stone and Shen [8] S3 | 0.00635 | 0.023 | 0.276 | 741–2341 | 16,706–91,269 | 0.118−0.669 | 0.55 |
| Stone and Shen [8] S4 | 0.00318 | 0.019 | 0.167 | 647–2692 | 12,637–52,561 | 0.092−0.385 | 0.55 |
| Ishikawa et al. [20] S1 | 0.004 | 0.0316 | 0.126 | 2137.188 | 22,546 | 0.209 | 0.29 |
| Ishikawa et al. [20] S2 | 0.0064 | 0.0632 | 0.101 | 3454.811 | 35,648 | 0.65 | 0.26 |
| Tsujimoto et al. [4] | 0.0015 | 0.002 | 0.75 | 153–634 | 10,191–42,388 | 0.103−0.429 | 0.44 |
| Fenzl [21] S1 | 0.00238 | 0.0024 | 0.992 | 647–1127 | 5096–8872 | 0.146−0.254 | 0.81 |
| Fenzl [21] S2 | 0.00238 | 0.0047 | 0.506 | 668–1773 | 5259–13,964 | 0.150−0.399 | 0.2 |
| Fenzl [21] S3 | 0.00238 | 0.0071 | 0.335 | 855–2692 | 6730–21,194 | 0.196−0.606 | 0.09 |
| Fenzl [21] S4 | 0.00238 | 0.0094 | 0.253 | 1043–2044 | 8219–16,096 | 0.235−0.460 | 0.05 |

In the present study, only one bed slope, a single value of roughness parameter having a fixed value of vegetation height, thickness, distribution pattern, spacing and density are considered. The dependency of drag coefficient on the above-mentioned parameter is expressed as

$$C_D = f_n(\mathrm{Re}_d, \mathrm{Re}_h, Fr, D/s, \lambda)$$

The developed relationships of drag coefficient ($C_\mathrm{D}$) are found to be in the power form with high value of coefficient determination ($R^2$) against $\mathrm{Re_d}$, $\mathrm{Re_h}$, Fr and $D/s$. Also, the developed relationship of drag coefficient ($C_\mathrm{D}$) is found to be in the exponential form against λ. The graphical relationship of the relationship is presented in Fig. 6.

It is observed that at lower vegetal density drag coefficient ($C_\mathrm{D}$) decreases with increase in both Reynolds numbers (i.e., $\mathrm{Re_d}$ and $\mathrm{Re_h}$) and increases with increase in Froude number. But, in case of higher vegetation density, $C_\mathrm{D}$ increases with increase in both Reynolds numbers (i.e., $\mathrm{Re_d}$ and $\mathrm{Re_h}$) and Froude numbers. It is also observed that $C_\mathrm{D}$ increases with increase in $D/s$ and decreases with increase in vegetation density at all values of Froude number. From Fig. 6, it is observed that values of $R^2$ from single regression of $C_\mathrm{D}$ with each independent parameters are very high which indicates that the developed model can work satisfactorily for evaluation of $C_\mathrm{D}$ by using multi-variable regression analysis.

Finally, the multi-variable regression model for drag coefficient has been developed as:

$$C_\mathrm{D} = 3.375 + 0.217{D/s}^{0.063} + 2.35\mathrm{Re_d}^{-0.03} + 0.998\mathrm{Re_h}^{-0.03} - 2.339\mathrm{Fr}^{-0.03} - 2.709e^{-0.01\lambda} \quad (5)$$

## 6 Results and Discussions

In this paper, three conventional models, i.e., Ishikawa et al. [20], Kothyari et al. [18] and Cheng [22], are used to compare with the present model. To check the efficacy of the present model, error analysis has been performed. The different parameters of error analysis, i.e., mean absolute deviation (MAD), mean absolute percentage error (MAPE) and root mean square error (RMSE), have been calculated as per given Eqs. (6)–(8) respectively.

$$\mathrm{MAD} = \frac{1}{n}\sum |(C_\mathrm{D})_\mathrm{Predicted} - (C_\mathrm{D})_\mathrm{Observed}| \quad (6)$$

$$\mathrm{MAPE} = \frac{1}{n}\sum \left|\frac{(C_\mathrm{D})_\mathrm{Predicted} - (C_\mathrm{D})_\mathrm{Observed}}{(C_\mathrm{D})_\mathrm{Observed}}\right| \times 100 \quad (7)$$

$$\mathrm{RMSE} = \sqrt{\frac{1}{n}\sum \frac{(C_\mathrm{D})_\mathrm{Predicted} - (C_\mathrm{D})_\mathrm{Observed}}{(C_\mathrm{D})_\mathrm{Observed}}} \quad (8)$$

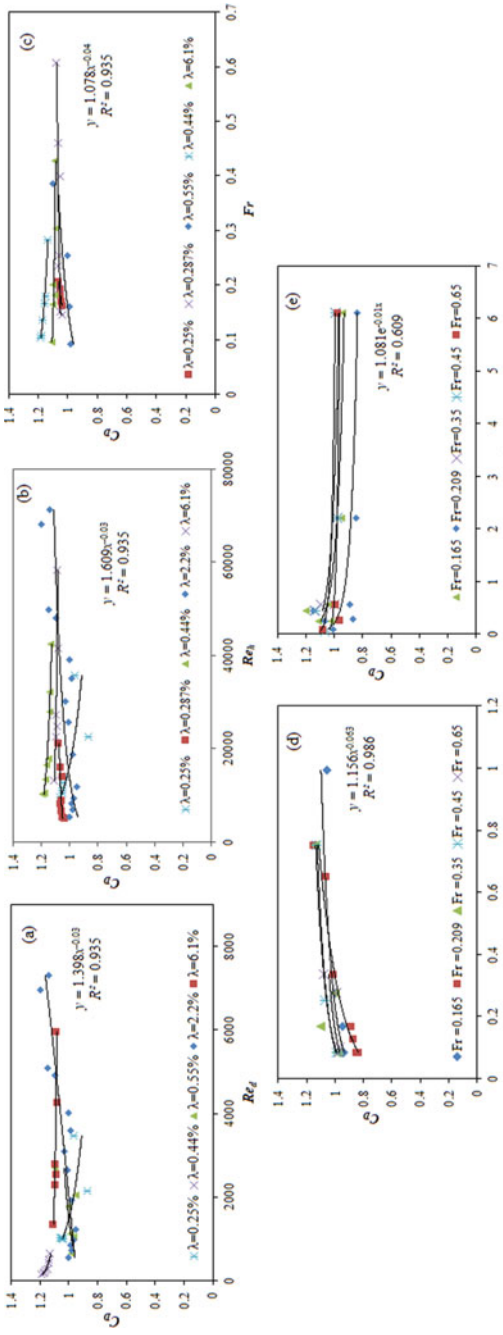


**Fig. 6** Plot between drag coefficient ($C_D$) and non-dimensional parameters **a** $C_D$ versus $Re_d$ **b** $C_D$ versus $Re_h$ **c** $C_D$ versus Fr **d** $C_D$ versus $D/s$ **e** $C_D$ versus $\lambda$

**Table 4** MAD, MAPE and RMSE results of different models used in this study

| Models | MAD | MAPE (%) | RMSE |
|---|---|---|---|
| Ishikawa et al. [20] | 0.25 | 20.80 | 0.27 |
| Kothyari et al. [18] | 1.28 | 122.16 | 1.19 |
| Cheng [22] | 2.17 | 226.74 | 8.89 |
| Present model | 0.04 | 3.48 | 0.05 |

From error analysis, it is observed that the present model is more efficient to predict drag coefficient than the previous models. From Table 4, it is found that the present model performs well with less error as compared to Ishikawa et al. [20], Kothyari et al. [18] and Cheng [22] models. The errors of MAD, MAPE and RMSE for present model are 0.04, 3.48% and 0.05, respectively which is less as compared to other conventional models.

## 7 Conclusions

Flow resistance is the most important hydraulic parameter of vegetated open channel flow. The various flow resistances like drag coefficient ($C_D$), Manning's roughness coefficient ($n$) and Darcy–Weisbach friction factor ($f$) are found to be more in vegetated open channel as compared to non-vegetated open channel.

The following conclusions are derived from the present study:

- The trend of the curves of the drag coefficient are expressed as power functions against $Re_d$, $Re_h$, Fr and $D/s$ and exponential function against λ. It is observed that at lower vegetal density drag coefficient ($C_D$) decreases with increase in both Reynolds numbers (i.e., $Re_d$ and $Re_h$) and increases with increase in Froude number. But, in case of higher vegetation density, $C_D$ increases with increase in both Reynolds numbers (i.e., $Re_d$ and $Re_h$) and Froude number. It is also observed that $C_D$ increases with increase of ratio $D/s$ and $C_D$ decreases with increase in vegetation density at all values of Froude number.
- Regression-based multi-variable model has been developed to predict the drag coefficient relating to Reynolds number (considering the stem diameter as characteristics length), Reynolds number (considering the flow depth as characteristics length), Froude number, Manning's $n$ and vegetation density under emergent rigid vegetation conditions. The model performed well with less error as compared to previous researchers' models.
- The different errors of MAD, MAPE and RMSE for present model are 0.04, 3.48% and 0.05, respectively, which is less as compared to other conventional models
- Additional research is desirable to validate the applicability of the rigid vegetation model developed in this study to flexible vegetation conditions.

**Acknowledgements** The authors would also appreciate the infrastructural support provided by National Institute of Technology Rourkela to carry out the present work. The previous researchers for their experimental data sets and researchers in the references are highly acknowledged.

## References

1. Brookes A, Shields Jr FD (1996) River channel restoration: guiding principles for sustainable projects, Wiley
2. Fathi-Moghadam M (2006) Effects of land slope and flow depth on retarding flow in non-submerge vegetated lands. J Agronomy 5(3):536–540
3. Goldman SJ, Jackson K (1986) Erosion and sediment control handbook, McGraw-Hill Education
4. Tsujimoto T, Kitamura T, Okada T (1991) Turbulent structure of flow over rigid vegetation-covered bed in open channels. KHL Progressive Report 1
5. Furukawa K, Wolanski E, Mueller H (1997) Currents and sediment transport in mangrove forests. Estuar Coast Shelf Sci 44(3):301–310
6. Meijer DG, Van Velzen EH (1999) Prototype-scale flume experiments on hydraulic roughness of submerged vegetation. In: Conference proceedings of the 28th international IAHR conference, Graz
7. Nepf HM (1999) Drag, turbulence, and diffusion in flow through emergent vegetation. Water Resour Res 35(2):479–489
8. Stone BM, Shen HT (2002) Hydraulic resistance of flow in channels with cylindrical roughness. J Hydraul Eng 128(5):500–506
9. Ghisalberti M, Nepf HM (2002) Mixing layers and coherent structures in vegetated aquatic flows. J Geophys Res Oceans 107(C2)
10. Dorcheh SAM (2007) Effect of rigid vegetation on the velocity, turbulence, and wave structure in open channel flows. Ph.D. Dissertation, Cardiff University, United Kingdom
11. Thom AS (1975) Momentum, mass and heat exchange of plant communities. Veget Atmos 57–109
12. Khuntia JR (2016) Effect of secondary current on flow prediction in an open channel flow, M. Tech dissertation, National Institute of Technology Rourkela, India
13. Khuntia JR, Devi K, Khatua KK (2016) Variation of local friction factor in an open channel flow. Indian J Sci Technol 9(46):1–6
14. Khuntia JR, Devi K, Proust S, Khatua KK (2018) Depth-averaged velocity and bed shear stress in unsteady open channel flow over rough bed. In: River flow 2018: 9th international conference on fluvial hydraulics, vol 40, issue no 05071, pp 1–8
15. Khuntia JR, Devi K, Khatua KK (2018) Prediction of depth-averaged velocity in an open channel flow. Appl Water Sci 8(6):1–14
16. Khuntia JR, Devi K, Khatua KK (2021) Turbulence characteristics in a rough open channel under unsteady flow conditions. ISH J Hydraul Eng 27(sup1):354–365
17. Panigrahi K (2015) Experimental study of flow through rigid vegetation in open channel. M. Tech (R) dissertation, National Institute of Technology, Rourkela, India
18. Kothyari UC, Hayashi K, Hashimoto H (2009) Drag coefficient of unsubmerged rigid vegetation stems in open channel flows. J Hydraul Res 47(6):691–699
19. Thompson AM, Wilson BN, Hustrulid T (2003) Instrumentation to measure drag on idealized vegetal elements in overland flow. Trans ASAE 46(2):295
20. Ishikawa Y, Mizuhara K, Ashida M (2000) Drag force on multiple rows of cylinders in an open channel. Grant-in-aid research project report, Kyushu Univ., Fukuoka, Japan

21. Fenzl RN (1962) Hydraulic resistance of broad shallow vegetated channels. Ph.D. Dissertation, University of California, Davis, California, USA
22. Cheng NS (2012) Calculation of drag coefficient for arrays of emergent circular cylinders with pseudo fluid model. J Hydraul Eng 139(6):602–611